Supporting Information

Enhanced detection of low-surface-charge nanoparticles via pressure regulation in solid-state nanopores

Tixi He, Yin Zhang*

Jiangsu Key Laboratory for Design and Manufacturing of Precision Medicine Equipment, School of Mechanical Engineering, Southeast University, Nanjing 211189, China.

* Corresponding author. E-mail: yin.zhang@seu.edu.cn

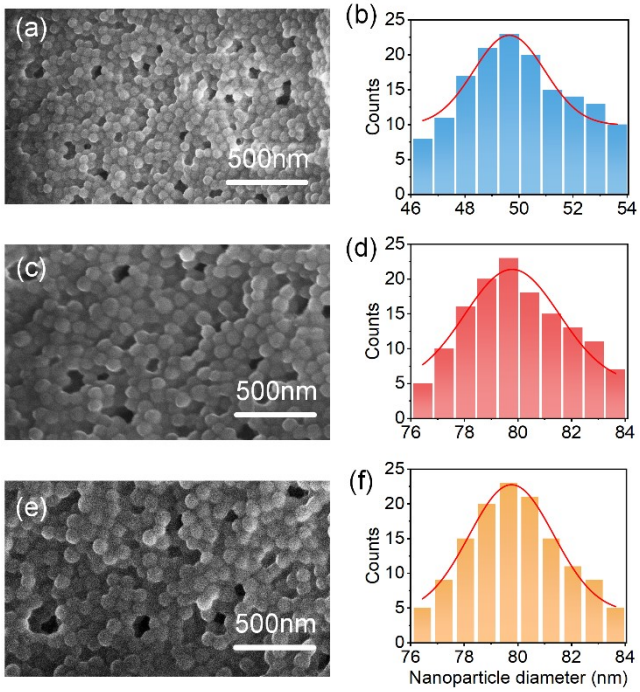

Fig. S1. SEM images of PS_{50} (a) and PS_{80} (c) and ZnO_{80} (e), (b, d, f) Statistical distributions show average diameters of 49.6±0.5 nm, 79.9±0.3 nm, and 80.1±0.1 nm, respectively.

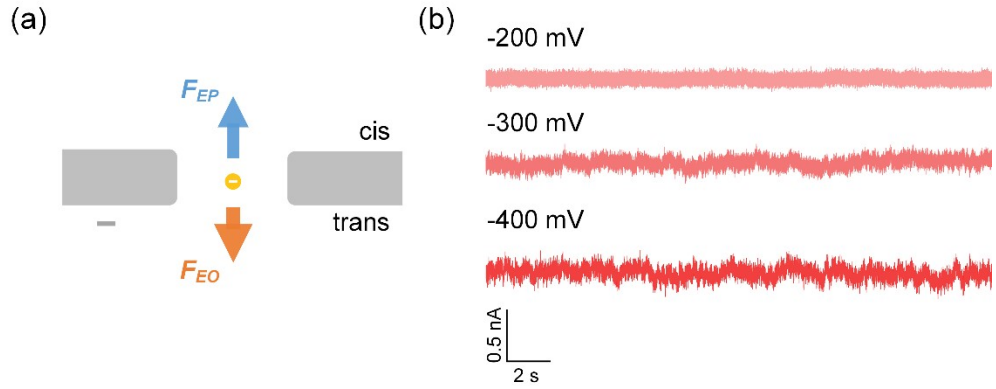

Fig. S2. (a) Schematic diagram of the force analysis of PS_{80} nanoparticles under the combined action of electrophoretic and electroosmotic forces. (b) The current-time traces of PS_{80} nanoparticles under the action of electroosmotic force at different voltages from -200 to -400 mV.

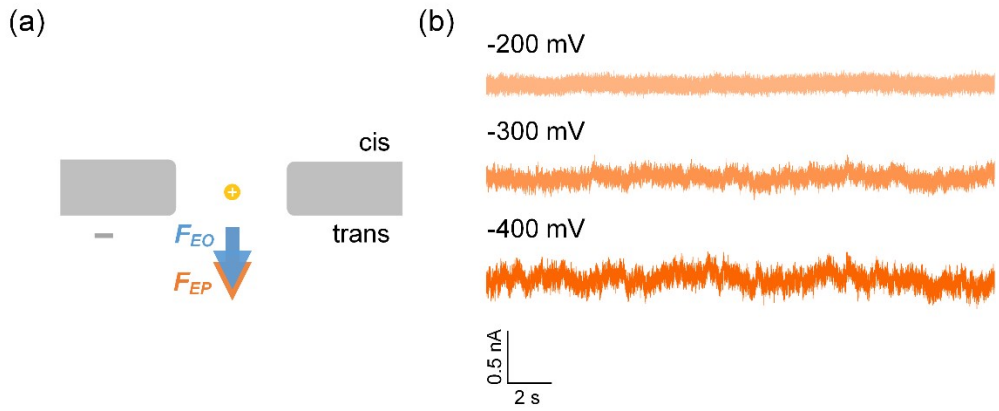

Fig. S3. (a) Schematic diagram of the force analysis of ZnO_{80} nanoparticles under the combined action of electrophoretic and electroosmotic forces. (b) The current-time traces of ZnO_{80} nanoparticles under the action of electroosmotic force at different voltages from -200 to -400 mV.

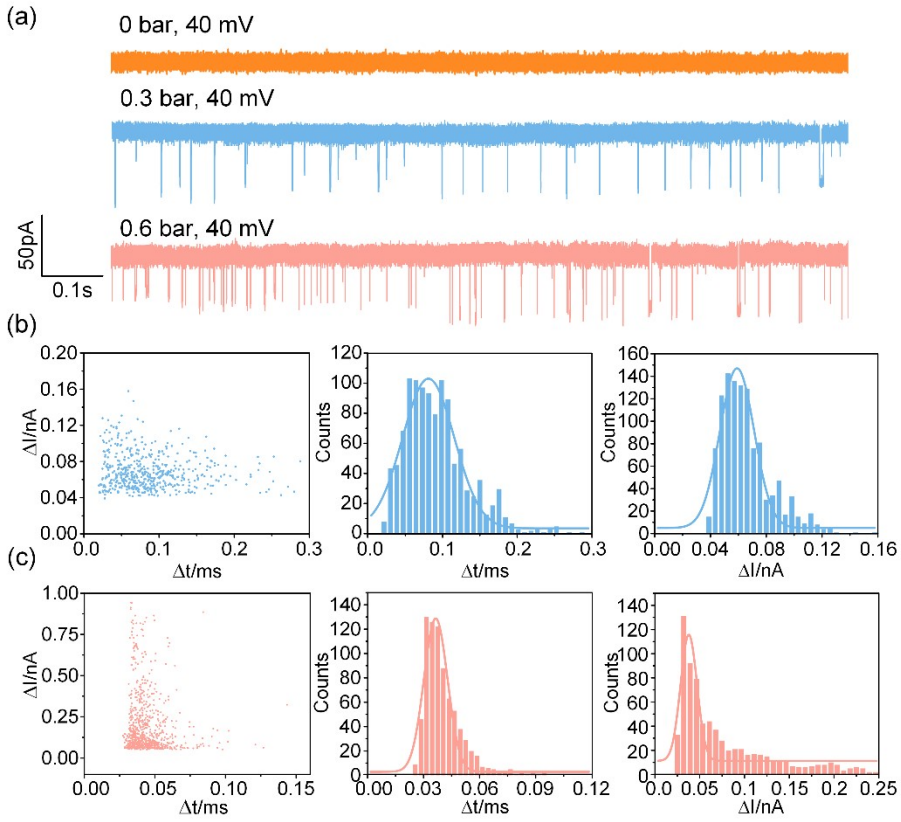

Fig. S4. PS_{50} nanoparticles translocation through a nanopore under different pressures using a 220 nm diameter nanopore in a 100 mM KCl buffer (pH 8.0). (a) Current-time traces at 0 bar, 0.3 bar, 0.6 bar (voltage at 40 mV). (b, c) Two-dimensional distribution between the dwell time and current blockade at 0.3 bar and 0.6 bar, respectively. The curved lines in the histograms of the dwell time and current blockade from Gaussian fitting.

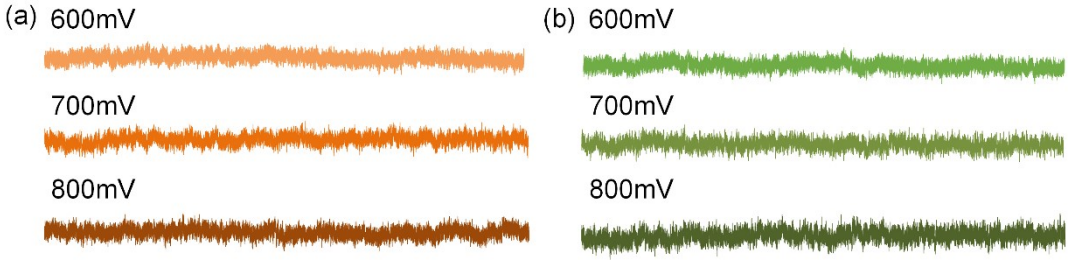

Fig. S5. Current-time traces corresponding to the translocation of nanopores by a single type of nanoparticles at different voltages from 600 to 800 mV in a 100 mM KCl solution. (a) PS_{80} nanoparticles. (b) ZnO_{80} nanoparticles. The concentrations of both types of nanoparticles were 10 pM.